Valence-electron excitations in the alkali metals

A. vom Felde,* J. Sprösser-Prou, and J. Fink
Kernforschungszentrum Karlsruhe, Institut für Nukleare Festkörperphysik, P.O. Box 3640, D-7500 Karlsruhe, Federal Republic of Germany
(Received 13 March 1989)

To study the dynamical response of the valence-electron gas in nearly-free-electron metals, we carried out an electron-energy-loss investigation on Na, K, Rb, and Cs. On polycrystalline samples we measured the volume plasmon dispersion, which showed strong deviations not only from the random-phase approximation, but deviations as well from the predictions of the current theories for Fermi liquids, including short-range exchange and correlation. In addition, anomalous dispersion of the plasmon half-width was found. Both results may be traced back to exchange and correlation effects not properly treated by the current Fermi-liquid theories. Furthermore, we observed the excitation of intraband transitions in Na and Rb, the dispersion of which yields the effective band mass for unoccupied states. The results for Na are at variance with recently published enhancement of the band mass for the occupied states. To elucidate the influence of band structure, measurements were also performed on a single-crystalline Na film and we observed the so-called zone-boundary collective state in Na.

I. INTRODUCTION

The alkali metals apart from Li are regarded as nature's closest realization of the free-electron-gas model and hence are claimed to be the metals understood best. Indeed, by de Haas–van Alphen measurements,[1] photoemission studies,[2] positron-annihilation investigations,[3] and optical experiments,[4–7] it seems well established that the alkali metals are nearly-free-electron (NFE) metals. However, the alkali metals have attracted new interest due to possible correlation effects which might seriously modify the free-electron-gas behavior. Recent experiments reporting on an enhanced magnetic susceptibility[8] of expanded liquid Cs and anomalous findings in positron annihilation spectra[9] of Cs indicated the importance of electron correlation at low valence-electron densities. A reinvestigation of the electronic structure of the alkali metals has also been stimulated by another phenomenon, the charge-density wave.[10] Its experimental evidence has been the subject of extensive discussions in the literature.[11–18] Stated that band-structure effects are small, the alkali metals offer a unique chance to study correlation effects of NFE systems at various electron densities. The understanding of the dynamics of a correlated free-electron system is considered to be of fundamental importance in metal physics.

The importance of exchange and correlation effects led us to an electron-energy-loss (EELS) investigation of the plasmon excitations in the NFE metals Na to Cs, since the existence of a plasmon is a direct consequence of the Coulomb interaction between the electrons.[19] We will show that the dispersion in plasmon energy shows strong deviations not only from the predictions of the random-phase approximation (RPA) but as well from more sophisticated Fermi-liquid theories. Especially, the negative volume plasmon dispersion of Cs indicates that exchange and correlation effects are much stronger than reflected by the current theoretical models. Parallel to the dispersion of plasmon energy, the dispersion of plasmon half-width shows substantial deviations from current theoretical calculations which likewise emphasizes the importance of exchange and correlation effects. Intra- and interband transitions provide information on the band structure. Consistently with the experimental results,[1–7] in the case of Na it turned out that band-structure effects are weak. There are only minor effects on the plasmon dispersion. The analysis of the dispersion of intraband transitions in Na yields an effective band mass close to one whereas the same investigation on Rb revealed a 25% enhancement of band mass. A band mass of close to one has also been deduced from the measurements of the dispersion of the zone-boundary collective states[20] (ZBCS) in Na. They have an extraordinarily low intensity relative to that of the volume plasmon. Nevertheless, we were able to observe it in Na for the first time. Part of this work has been published previously.[21,22]

II. THEORETICAL BACKGROUND

Plasmons are a direct consequence of the interelectronic Coulomb interaction in solids. A widely used first approach to tackling this many-body problem is the RPA,[19] a mean-field theory restricted to long-range interactions and exact only in the limit of high electron density $r_s \ll 1$, a case not very realistic for ordinary metals with $2 < r_s < 6$. (r_s is the Wigner-Seitz radius for electronic spacing, expressed in Bohr radii.) In spite of its shortcomings, the RPA was successful in describing many experimental findings. For instance, it has explained many experimental data[23] on the volume plasmon dispersion $E(q)$ with momentum transfer q:

$$E(q)=E(0)+(\hbar^2/m)\alpha_{\mathrm{RPA}}q^2+O(q^4)$$

where m is the electron mass and the dispersion coefficient is given by

$$\alpha_{\mathrm{RPA}}=\tfrac{3}{5}[E_F/E(0)] ,$$

E_F being the Fermi energy. Such a positive quadratic dispersion with dispersion coefficient close to the one predicted in the RPA has indeed been observed in many earlier experiments.[23]

A shortcoming of the RPA is the absence of any damping mechanism, resulting in an infinite plasmon lifetime for momentum transfers smaller than the critical momentum transfer q_c where the plasmon curve reaches the range of single-particle excitations. The situation has been improved by introducing a simple, phenomenological relaxation time in a particle-conserving manner,[24] yielding the so-called Lindhard-Mermin (LM) function for the response of a free-electron gas. The RPA has been further improved considerably by the inclusion of short-range exchange and correlation effects by means of local field corrections (LFC), describing the effect of an exchange-correlation hole comoving with the electron. We do not want to discuss the various LFC's we are going to use in a subsequent comparison of experimental and theoretical data on the volume plasmon dispersion. We merely note that the common effect of all LFC's is to lower the dispersion coefficient the more, the lower the electron density.[25]

So far in this section, we have discussed the electrons as free and have neglected the effect of the ion cores. First, the core electrons constitute a polarizable background, which tends to screen the plasma oscillation. Since the excitation energies for core electrons are by far higher than the plasmon energy, the polarizability of the core electrons can be well approximated by a static polarizability contribution added to the LM function.[26]

Second, the effect of the nonhomogeneous crystal potential caused by the ion cores leads to interband transitions within certain ranges of momentum transfer thus possibly shifting the plasmon energy and changing the dispersion coefficient.[27] Experimental evidence for sudden changes in the slope of the plasmon dispersion curve was claimed by several authors.[28–31]

Third, the presence of ion cores modulates the valence-electron density, thus allowing plasmons to decay into interband transitions, which limits their lifetime even in the long-wavelength limit, in the absence of crystal defects and at zero temperature. The plasmon full width at half maximum is given by[27]

$$\Delta E_{1/2}(q)=\Delta E_{1/2}(0)+(\hbar/m)\beta q^2 ,$$

where $\Delta E_{1/2}(0)$ is the width at $q=0$ and β is the dispersion coefficient of the plasmon width. The calculation of the dielectric response in the reduced translational symmetry of a crystal is a laborious problem and has been carried out in an approximative manner for a few metals only.[32] Using the NFE approximation, it turns out that the plasmon half-width depends on those Fourier components of the pseudopotential the corresponding wave vectors of which are able to couple the plasma oscillation to the continuum of electron-hole pair excitations. For wave vectors q greater than the critical wave vector q_c, the aid of a reciprocal lattice vector is not needed since now the plasmon can decay directly into particle-hole excitations. This Landau damping shows up as a strong increase of the plasmon half-width[23] for $q>q_c$.

Finally, the periodic crystal potential leads to a gap in the electron-hole pair excitation continuum. Electronic states originally located in the energy region of the gap are now shifted to the gap edges, leading to van Hove singularities. Transitions from the occupied part of the band into states close to these singularities, i.e., a combination of intra- and interband transitions, cause the ZBCS in the loss function.[20]

III. EXPERIMENT

Thin polycrystalline films were produced by thermal evaporation of the alkali metals on 50–100 Å thin polymer substrates under ultrahigh vacuum (UHV) conditions provided by a preparation chamber attached to the EELS spectrometer. The thickness of the alkali films, monitored by a quartz gauge, was chosen to be about 500 Å. During the evaporation, the substrate was held at room temperature and the deposition rate was 2–5 Å/s. Characterization of the samples was carried out in UHV at liquid-nitrogen temperature. From the diffraction patterns we deduced that the films were fine grained, having a grain size of about 200 Å. Single-crystal Na films were obtained likewise by thermal evaporation on MgO single-crystal films, whereas all the other parameters (thickness, deposition rate, etc.) remained unchanged. Prior to evaporation, the MgO film was heated for 5–10 h up to 600 °C in order to remove surface contaminants. Epitaxial growth on the single-crystal surface resulted in single-crystalline Na films with a mosaic spread of about 5°. The MgO substrates were produced by thermal evaporation from sintered MgO tablets on LiF covered NaCl single crystals held at a temperature[33] of 420 °C. The thickness was 700 Å, the deposition rate was 5 Å/s. The LiF coverage had a thickness of less than 300 Å. It was grown epitaxially by thermal evaporation on freshly cleaved NaCl crystals held at 360 °C with a deposition rate of 10 Å/s. Finally, the MgO films were floated off the NaCl substrate in distilled water, which made the LiF coverage dissolve completely. The thickness of the MgO substrate was checked by Rutherford backscattering measurements. All alkali metal films were characterized by electron diffraction and core-level spectroscopy. Within error limits, no oxidation of the films was detected. The polymer and MgO substrates exhibited a good transparency in the spectral region (0–8 eV) crucial for the detection of valence-electron excitations in the alkali metals. The spectra were taken in UHV at liquid-nitrogen temperature with a high-resolution 170-keV EELS spectrometer described elsewhere.[22] The energy and momentum resolution were chosen to be 0.16 eV and 0.04 Å,[1] respectively.

IV. RESULTS

A. Volume plasmon dispersion

Figure 1 shows typical energy-loss spectra for various momentum transfers q taken on a Na film. The uppermost spectrum reveals at low energy two surface plasmons, reflecting the electron oscillations on the metal-substrate and on the metal-vacuum interfaces, respectively. The sharp line slightly below 6 eV represents the volume plasmon loss. At $q=0.3$ Å^{-1} the surface plasmon intensities have disappeared from the spectra and one is left with a broadened volume plasmon excitation. At even higher q, the plasmon line is rapidly broadened due to Landau damping (q_c for Na is about 0.75 Å^{-1}), whereas multiple scattering intensities increasingly contribute to the spectra. Visibly, double scattering creating a plasmon with $q=0$ and a quasielastic event with q equal to that set by the spectrometer seriously obscures the spectra in Fig. 1 for $q>0.7$ Å^{-1}. However, since Na and K volume plasmons show a dispersion, double scattering contributions at large q, occurring at the plasmon energy for $q=0$, can easily be subtracted from the shifted plasmon line. For Rb and Cs the problem was more severe due to the weak dispersion of their plasmons (see below) causing the plasmon line and the double scattering contributions to occur at about the same energy. The appearance of double scattering in these cases was realized by a sudden decrease in volume plasmon linewidth and a corresponding sudden increase of the plasmon loss intensity with increasing q. Data in this q range have been rejected in our analysis.

Figures 2(a), 2(b), 2(c), and 2(d), which are plots of the plasmon energy versus the square of the transferred momentum in the excitation process, comprise our results on the volume plasmon dispersion. Comparison of our data with previous measurements of Na (Refs. 28 and 34–37) and K (Refs. 28 and 35) reveal good agreement of the plasmon energies within about 0.1 eV. For Rb and Cs there are no previous measurements of the plasmon dispersion. We have implemented a different way[38] of determining the dispersion coefficient by fitting the data with a function of the form

$$E(q)=A+Bq^2+Cq^4$$

(thin solid line) up to the critical wave vector q_c. From the parameter B dispersion coefficients α could be derived and are given in Table I. The other curves describe theoretical calculations. The uppermost dash-dotted line gives the plasmon dispersion using the LM function.[24] Starting at the same energy value, the dashed line represents the RPA with inclusion of a LFC by Vashishta and Singwi[39] (VS) which reduce the plasmon dispersion at low q. The solid line resulted after additional inclusion of a core polarization term.[26] The core polarizabilities were taken from experimental work on alkali metal ions[40] because for the metallic state, there were none available. The inclusion of the core polarizability lowers the long-wavelength plasmon energy and brings the theoretical result closer to the experimental value.

To elucidate the influence of band-structure effects, we also carried out, with improved statistics, dispersion measurements on a Na single crystal. Figure 3 shows the difference of the plasmon energy measured with q along the [110] and the [100] orientations, respectively. The plasmons with wave vector q parallel to the [110] direction have higher energies than those with q parallel to

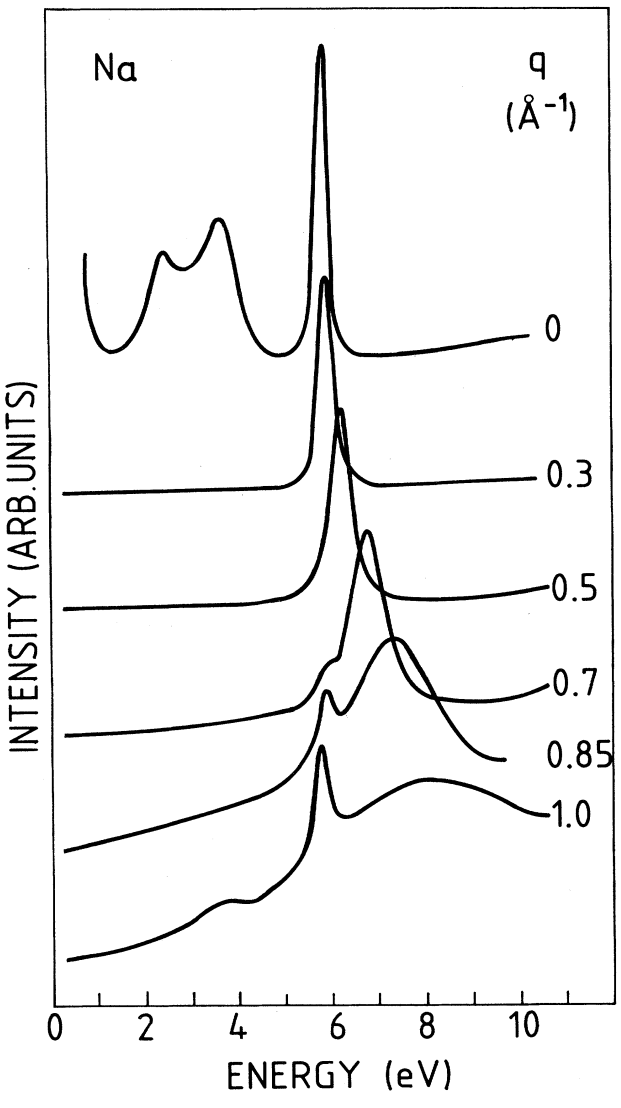

FIG. 1. Experimental energy-loss spectra of Na for different momentum transfers, demonstrating surface plasmons, the volume plasmon dispersion, and the onset of double scattering contribution at high q ($q>0.7$ Å^{-1}).

TABLE I. Data used from the literature: Wigner-Seitz radius r_s in units of Bohr radii, Fermi wave-number k_F and Fermi energy E_F, critical wave number q_c (defines where plasmon enters particle-hole continuum), plasmon dispersion coefficient α_{RPA} from theoretical calculations in RPA. Measured values: Plasmon dispersion coefficient α_{expt} from parameter B in a fit $E_p(q)=A+Bq^2+Cq^4$ to the experiment, full width at half maximum of the plasmon $[\Delta E_{1/2}(0)]$ in the long-wavelength limit, dispersion coefficient β from experimental half-width dispersion, effective electron mass m^* in the unoccupied part of the valence band in units of free-electron mass, damping parameter Γ used in a least-squares fit to obtain the band mass, given at two different wave numbers.

	r_s/a_0	k_F (Å^{-1})	E_F (eV)	q_c (Å^{-1})	α_{RPA}	α_{expt}	$\Delta E_{1/2}(0)$ (eV)	β	m^*/m	Γ (eV)	at q (Å^{-1})
Na	3.93	0.92	3.24	0.75	0.32	0.17	0.28	0.11	1.05 (±0.04)	0.35	0.25
										0.42	0.40
K	4.86	0.75	2.12	0.65	0.29	0.075	0.24	0.30			
Rb	5.20	0.70	1.85	0.62	0.28	0.045	0.39		1.25 (±0.06)	0.18	0.17
										0.31	0.31
Cs	5.62	0.65	1.59	0.59	0.27	−0.18	0.77				

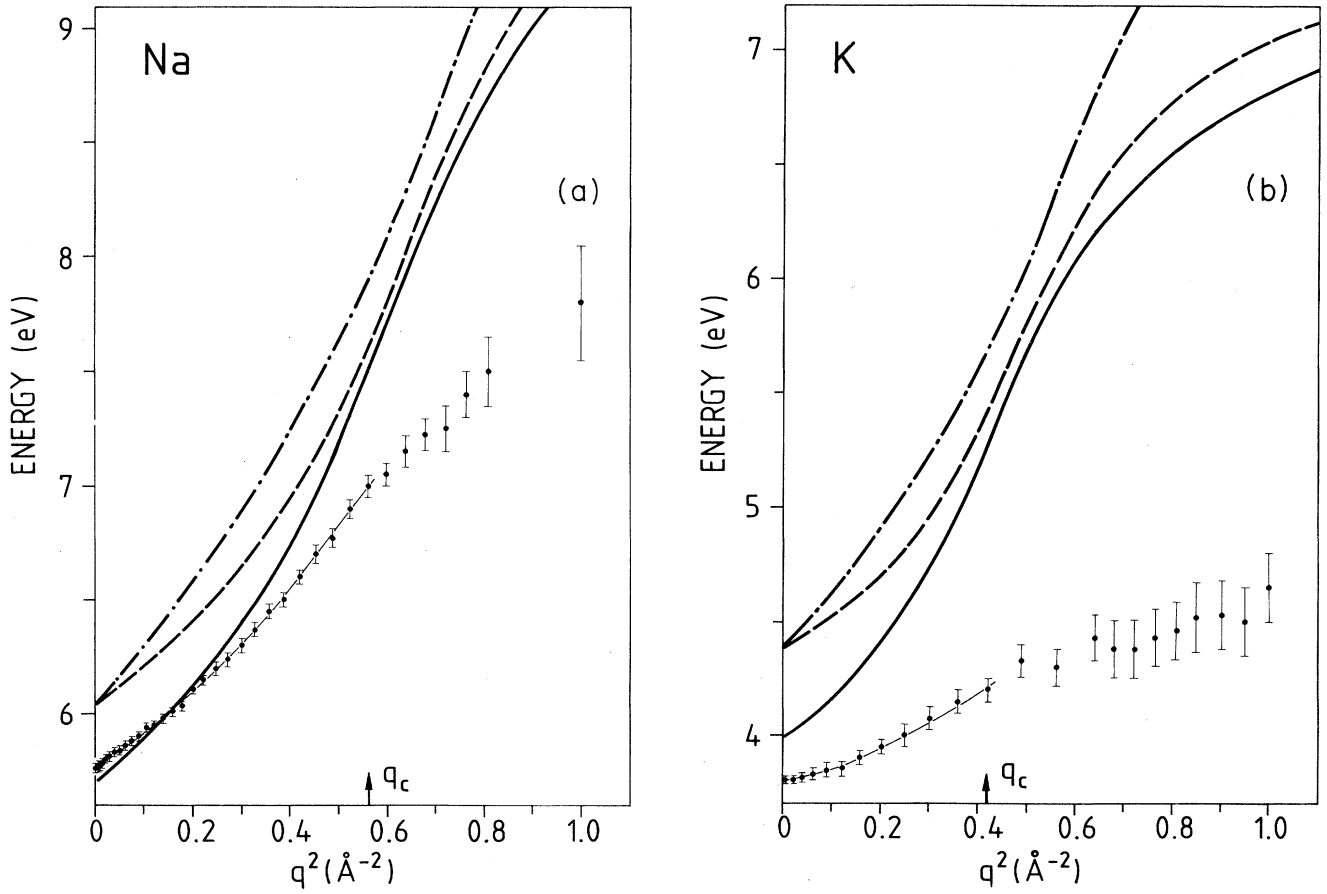

FIG. 2. Experimental plasmon dispersion (points with error bars) for polycrystalline Na (a), K (b), Rb (c), and Cs (d), compared to theoretical curves. Dash-dotted line: Lindhard-Mermin function. Dashed line: the same with inclusion of a local field corrrection by Vashishta and Singwi. Solid line: Core polarizability included. The experimental data have been fitted with a function of the form $E(q)=A+Bq^2+Cq^4$ (thin solid line) up to the critical wave number q_c.

[100]. The overall difference in plasmon energy measured in different directions remains less than 40 meV for $q < q_c$

B. Volume plasmon halfwidth

Figure 4 provides the measured plasmon half-widths as a function of the momentum transfer q. The reader should note that the abscissae are scaled in different powers of q. In Table I we report the starting half-width $\Delta E_{1/2}(0)$ as well as the dispersion coefficients β. For Na and K the data are not very different from what has been measured by other authors on NFE metals.[28,36,37] We found a positive quadratic dispersion which changes more or less abruptly at the critical wave vector q_c (least-squares fits of straight lines are indicated by the thin solid lines). One should notice that the linewidth in K increases much faster than in Na (note the different energy scales). Whereas in the long-wavelength limit the plasmon widths are almost identical, at about q_c the plasmon width of K is about twice as large as that on Na. In the case of Rb, it turned out that the data on plasmon half-width did not fit $\Delta E_{1/2}(q) = \Delta E_{1/2}(0) + \beta q^2$. For $q < q_c$ best agreement with a straight line was obtained in a plot $\Delta E_{1/2}(q)$ versus q^x with $x = 1.5 \pm 0.2$. The most striking case is given for the metal having the highest r_s value, i.e., for Cs, where the data show a perfect linear relationship between plasmon half-width and wave vector. This is in sharp contrast to what has been known so far, namely, that the width of a plasmon line has a positive quadratic dispersion. It is interesting to note that the linear dispersion extends beyond q_c.

C. Intraband transitions and ZBCS

When performing measurements with small statistical error bars on Na and Rb in the energy range below the plasmon, we detected a comparatively weak structure with strong dispersion in momentum transfer. This structure can be ascribed to intraband transitions. To give examples, Fig. 5 shows two experimental spectra for each of the two metals, taken at different momentum transfers (solid lines: least-squares fits within the LM model). The observation of the intraband loss intensity is limited in q space, towards zero energy by the tail of the intense elastic peak (when q is below 0.1 Å^{-1}) and to-

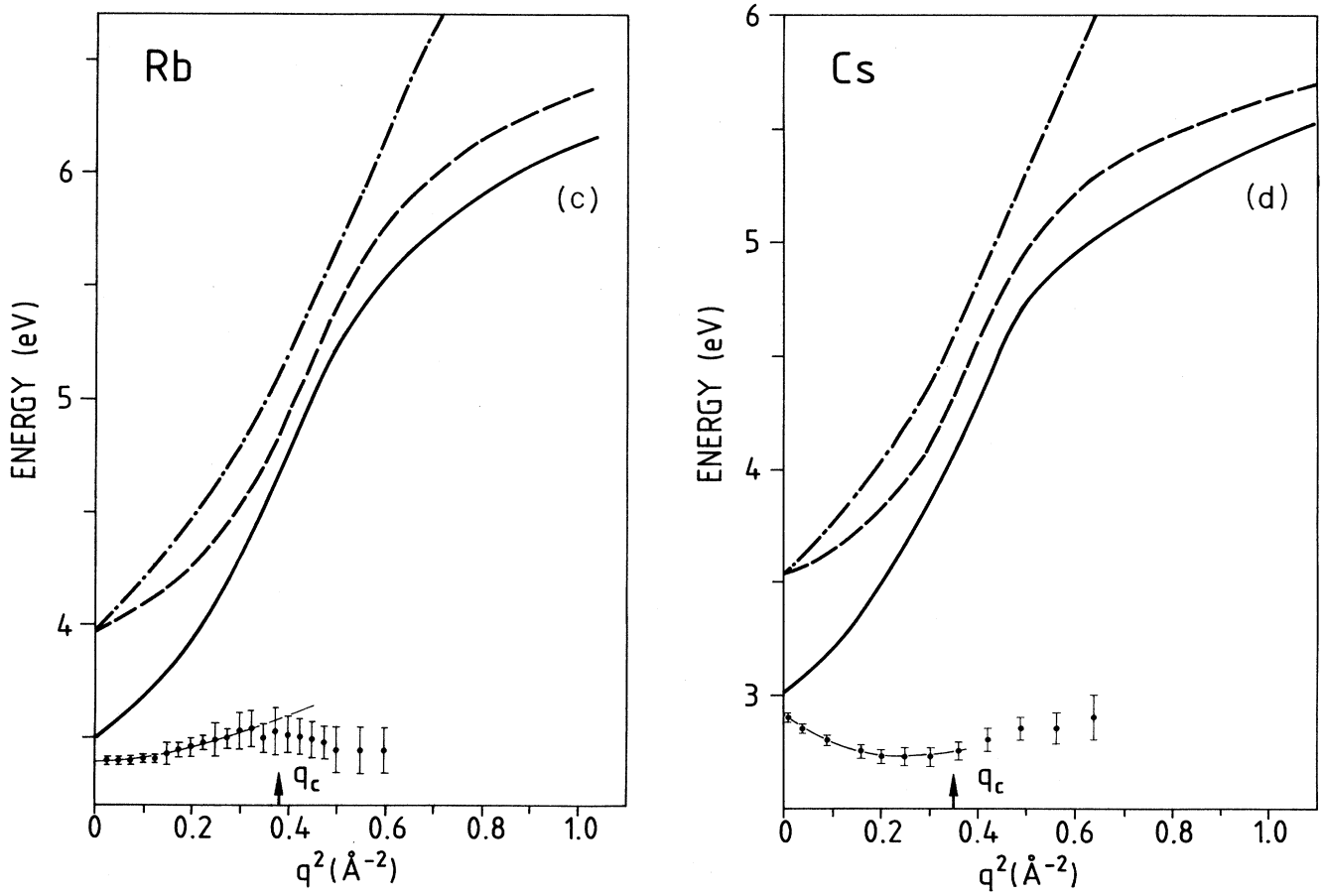

FIG. 2. (*Continued*).

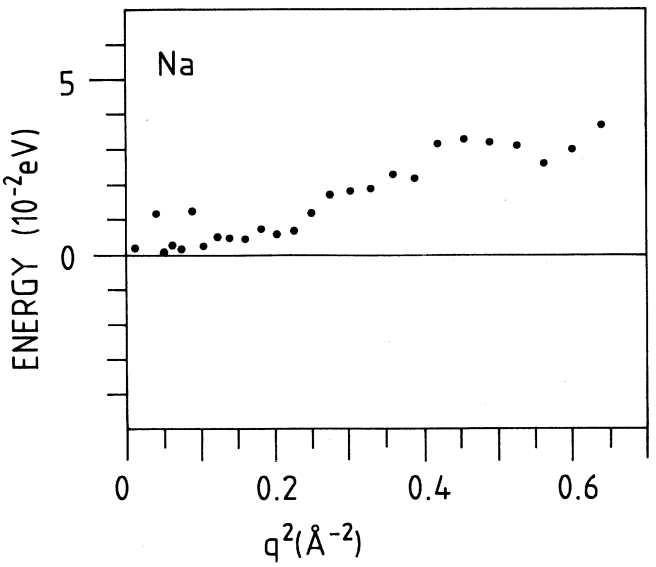

FIG. 3. Difference of plasmon energy, measured on a Na single crystal with q||[110] and q||[100], respectively.

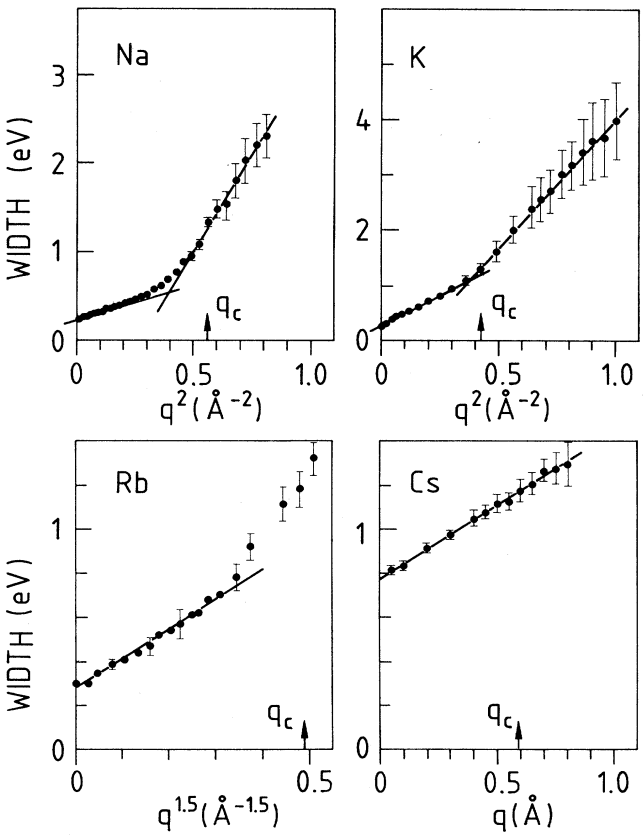

FIG. 4. Dispersion of the plasmon half-width as measured on the four alkali metals, plotted vs different powers of momentum transfer q. The straight lines represent least-squares fits to the data points. For Na and K the data have been fitted below and above q_c.

wards plasmon energy by the volume plasmon tail (when q is above ~ 0.75 Å^{-1}).

In Fig. 6 the same type of spectrum is plotted, but for the Na single crystal. Both the solid and the dashed lines represent measured spectra for q||[110] and q||[100], respectively. For q||[110] one finds an additional small intensity, which can be identified as originating from the ZBCS as will be discussed below. Maxima due to ZBCS could be detected for $0.3 \leq q \leq 0.75$ Å^{-1}. The dispersion of these ZBCS's is shown in the inset of Fig. 6.

V. DISCUSSION

A. Volume plasmon dispersion

Figure 2 provides a comparison between the measured volume plasmon dispersion and calculations for three different models. What makes experiment deviate so much from calculations? There has been a considerable debate as to how band-structure effects enter into the

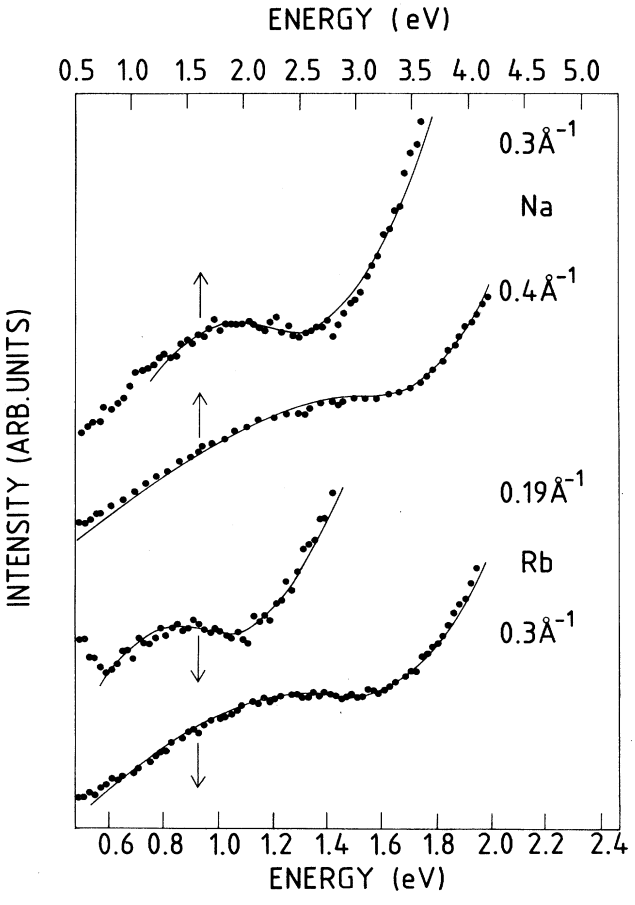

FIG. 5. Intraband transitions in the loss spectra at various momentum transfers. Upper spectra and energy scale for Na, lower ones for Rb. Lines from least-squares fits of the loss function Im$(-1/\epsilon)$, where ϵ is the Lindhard-Mermin dielectric function including local field corrections by Vashishta and Singwi (Ref. 39).

plasmon dispersion. Some authors[28–31] claimed that the dispersion at low q is lowered by band-structure effects and reported that observation of a discontinuity in the slope of the dispersion curve of Al. However, in this case it was not clear why the dispersion curves of Al measured on single crystals with q in different high-symmetry directions only start to deviate from one another at high q. On the other hand it was stated[27] that band-structure effects should affect the dispersion coefficient in the high-q range. As a result, experimentalists switched over to describe measured dispersion curves in terms of two dispersion coefficients for the low- and high-q regions.[31]

In our opinion the above-mentioned interpretations have to be doubted in particular because for the same metal, e.g., Al, several q values for the discontinuity have been reported (0.37 Å^{-1} in Ref. 28, 0.57 Å^{-1} in Ref. 30, 0.75 Å^{-1} in Ref. 31). Hence we looked very carefully for the occurrence of discontinuities in the dispersion curves of the alkali metals, and we reinvestigated the case of Al,[38] but we found none. Different from all analyses of plasmon dispersion data carried out so far, we describe our curves in terms of a power law as is suggested by the RPA, including a fourth-order term q^4 beside the quadratic q^2. As can be inferred from Fig. 2 the data are well fitted by this power law, indicating that there is no need for two dispersion coefficients. The claimed discontinuities seem to be an artifact of the analysis, occurring when the dispersion curve is measured with too coarse a q mesh or when the data points show considerable statistical fluctuations.

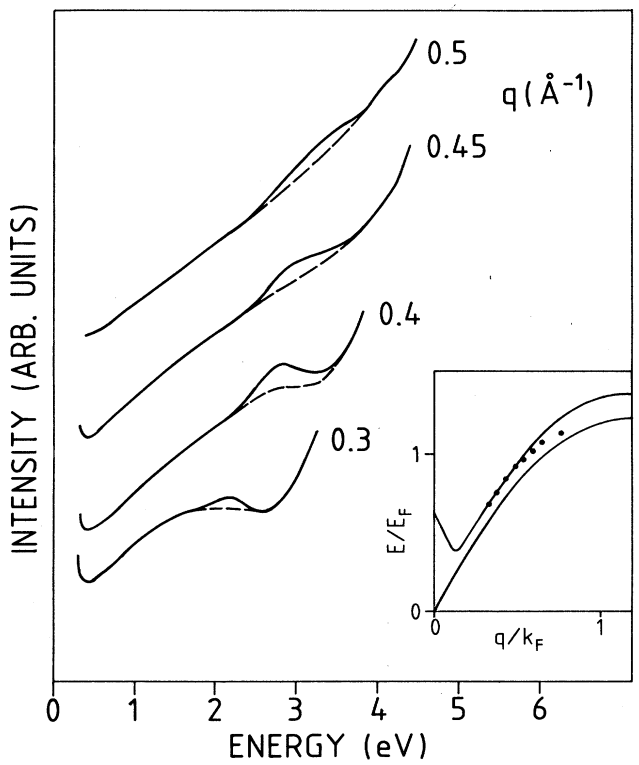

FIG. 6. Comparison of the Na spectra in the low-energy region (see Fig. 5) for $\mathbf{q}\|[110]$ (solid lines) and $\mathbf{q}\|[100]$ (dashed lines). The difference in the intensities is due to the excitation of the Na zone-boundary collective state. The dispersion of these excitations in the gap between intraband and interband transitions is shown in the inset.

The question remains, whether the dispersion curve is affected as a whole by band-structure effects. In the case of Na we found a difference in the dispersion of plasmon energy for wave vectors pointing along [110] and [100]. In a simple picture neglecting exchange and correlation, the plasmon dispersion is a measure of v_F^2, the Fermi velocity squared. In the direction of the nearest zone boundary, the Fermi surface forms bottlenecks and v_F^2 differs from any other nonequivalent direction. However, the extremely small difference in the plasmon dispersion found for q along different high-symmetry directions and also the weakness of the ZBCS (see below) points to only weak band-structure effects in Na. Unfortunately, no such data could be obtained for the other alkali metals. We only succeeded in growing single crystals of K on MgO but not with a simple orientation (K[310] on MgO[100]). Concerning the heavier alkali metals, one might expect an influence of electron transitions to unoccupied $3d$ states, which come close to the Fermi level when going from K to Cs.[41,42] However, the s-d matrix element is very small, and we have not observed any interband transitions in the energy range below 10 eV. Another fact which votes against any considerable influence of interband transitions is that the volume plasmon energy at $q=0$ is close to its free-electron value when core polarization is included. Interband transitions are known to renormalize the plasmon energy if they are strong and close in energy to the plasmon. The strong renormalization of the Ag plasmon energy is a famous example.[23]

Previous measurements of the plasmon dispersion in simple metals always showed a positive, quadratic dispersion. Rb is the first metal to show almost no dispersion at all, see Fig. 2(c). The deviation becomes even more marked in the case of Cs, which exhibits a plasmon with a negative dispersion. Deviations not only occur with respect to the RPA (which is to be expected), but to improved theories as well. This is presented in Fig. 7 where we supply the experimental dispersion coefficients normalized to the RPA values versus r_s. The solid line corresponds to calculated values using RPA and static LFC's of VS included (other static LFC's gave similar results). The dashed line represents the dynamic LFC proposed by Dabrowski.[43] It is evident that the experimental results deviate strongly from the predictions of current Fermi-liquid theories. Particularly, the deviations increase with r_s. We can take r_s as a rough measure of the strength of correlation effects. The ratio of the potential energy of an electron $V\sim 1/\epsilon r_s$, to its kinetic energy $E_{\text{kin}}\sim 1/r_s^2$, i.e., $V/E_{\text{kin}}\sim r_s/\epsilon$ gives an indication of the strength of the electron-electron correlation. Using r_s/ϵ instead of r_s on the abscissa of Fig. 7 would even enhance the discrepancies.

Now we turn to the discussion of the influence of core electrons on plasmon dispersion. The bold lines in Fig. 2 give the result of a LM calculation with inclusion of a

constant static term added to the Lindhard function to account for core electron polarization. The resulting dispersion coefficients, normalized to the RPA values, are shown by the open circles in Fig. 7 not yet discussed. The added polarizabilities are probably somewhat too high, because they were measured not in metal but in alkali halides where the conduction bands are empty. Although the added term is constant, its effect on plasmon dispersion is q dependent, see Fig. 2. This is due to the LFC. While for high q the dispersion appears to be influenced mainly by the LFC, for low q the LFC is of minor importance, i.e., the core electrons counteract the local field which itself tends to reduce the dispersion coefficient. Hence, with inclusion of the core polarization, the deviations between experimental results and theoretical predictions are even more pronounced. This is in principle the same as discussed above when replacing r_s with r_s/ϵ.

With Fig. 8 we turn now to a comparison, not only of the dispersion coefficient, but of the entire experimental dispersion curve with theory. Different from Fig. 2, the plasmon energy is now normalized to its long-wavelength energy and the abscissa is linear in momentum transfer. The downward triangles (Na), upward triangles (K), circles (Rb), and diamonds (Cs) reflect the measured data. The solid lines resulted from a calculation of the plasmon dispersion in an electron liquid with various densities ($r_s = 2-20$) including the LFC of Singwi *et al.*[44] (this is the LFC preceding the LFC of VS). This LFC is noticeable, since for $r_s > 6$ it produces a negative plasmon dispersion. We mention, however, that this LFC does not fulfill the exactly valid self-consistency conditions as well as the LFC by VS does. Nevertheless, we have chosen the LFC of Singwi *et al.*[44] because it is the only one where the entire dispersion curves have been calcu-

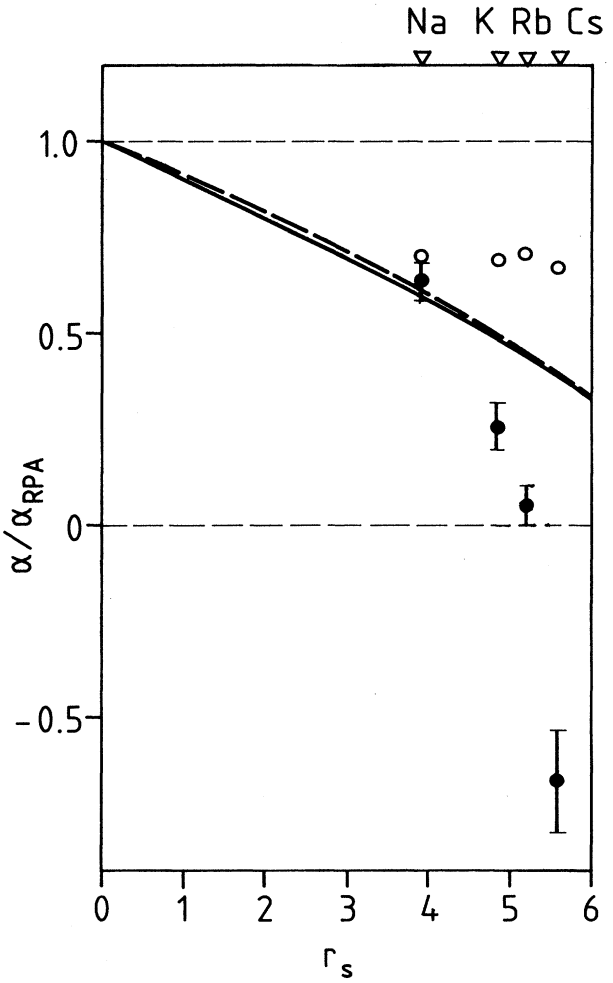

FIG. 7. Volume plasmon dispersion coefficient normalized to the dispersion coefficient in RPA vs the Wigner-Seitz radius r_s. The solid circles with error bars represent the results from our measurements. The solid (dashed) line gives the dispersion coefficient calculated with inclusion of a local field correction by Vashishta and Singwi (Ref. 39) [by Dabrowski (Ref. 43)], the open circles give the dispersion coefficient when core polarization is accounted for.

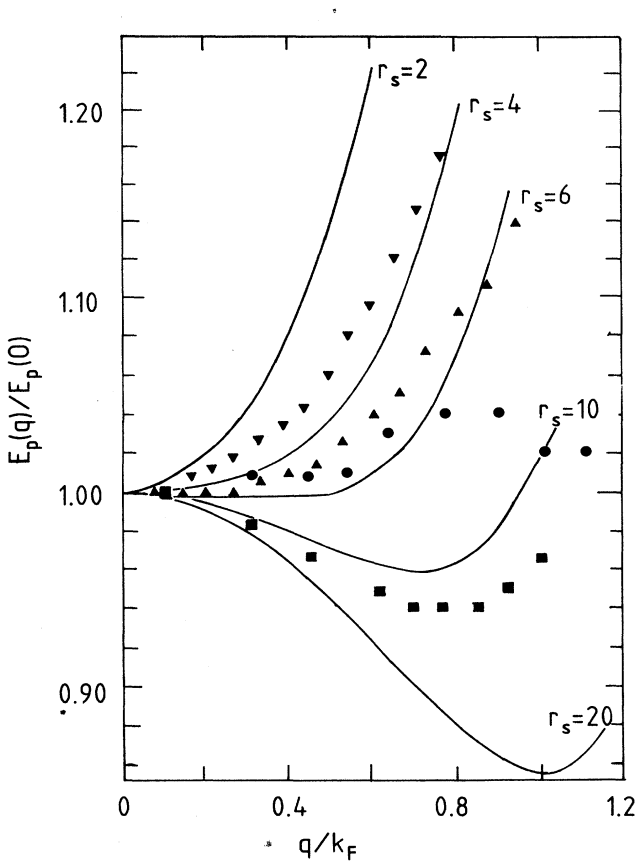

FIG. 8. Volume plasmon dispersion normalized to the plasmon energy at $q = 0$. The symbols represent the experimental data for Na ($r_s = 3.93$, downward triangles), K ($r_s = 4.86$, upward triangles), Rb ($r_s = 5.20$, circles), and Cs ($r_s = 5.62$, squares). The solid lines give the theoretical plasmon dispersion of Singwi *et al.* (Ref. 44) for various r_s.

lated up to exceedingly low electron densities ($r_s = 20$). Astonishingly, the shapes of the theoretical and experimental curves are quite similar. Evidently, this agreement is qualitative but by no means quantitative. A theoretical curve fitted to the measured values of Cs would yield $r_s = 12$, corresponding to a hypothetical metal with one-eighth of the Cs valence-electron density.

We extrapolated the LFC of VS, too, and calculated the entire dispersion curves. The results are sensitive to the kind of extrapolation chosen, and it is not guaranteed that after application of a specific extrapolation the self-consistency conditions are still fulfilled. However, what can certainly be said, is that using this LFC, the required r_s to describe the Cs result would be even higher than in the case of the LFC by Singwi *et al.*[44] This means that in spite of the improvements achieved on using the improved LFC, the discrepancy between experiment and theory even increases.

To compare our data with the predictions of Fermi-liquid theories, we picked out the LFC of VS, which is the most widely used static LFC. The LFC of Dabrowski[43] is based on the VS LFC and has been chosen to provide also a comparison to a dynamical LFC. We emphasize that the substantial deviations between experimental data and theoretical predictions remain, irrespectively of the specific choice of LFC, i.e., at the time being there is no LFC, neither static nor dynamic, able to explain the experimental findings. One may perform a Kramers-Kronig analysis of the measured loss functions in order to extract a LFC from the obtained complex dielectric function. This was carried out in the case of Al and Na.[36] One should note that this procedure will mathematically work in any case, but in general the obtained LFC will not satisfy the self-consistency conditions.

Independent of our measurements, a theory has been established by Taut[45] which offers an alternative explanation, involving both band-structure and correlation effects. It is based on the correlation induced peak[46] near $2k_F$ in the static structure factor of the homogeneous electron gas, backfolded by a reciprocal lattice vector with the absolute value close to $2k_F$, thus yielding an anomaly in the plasmon dispersion of Li, Rb, and Cs at q below $0.5q_F$. Qualitative agreement is obtained, but not a quantitative one.

If correlations become very strong in a metal the electron system condenses in a lattice, the Wigner crystal.[25,47] Recent calculations[48] yield a value of $r_s = 100 \pm 20$ for this transition. (For comparison, the hypothetical r_s value derived from the fit of theoretical curves to the plasmon dispersion of Cs was $r_s = 12$.) Although Cs is a metal one may interpret the negative dispersion by an incipient crystallization of the electron system. What should the plasmon dispersion in a Wigner crystal look like? If the electrons have condensed to form a lattice the plasmon is the analogue to an optical phonon of an ion lattice.[49] An optical phonon exhibits a negative dispersion, as observed in the case of the Cs plasmon. A reduction of the plasmon energy is equivalent to a reduction of the restoring forces for a certain wavelength and hence an indicator for the system's tendency to generate a nonhomogeneous electron density distribution by itself. Finally, it is interesting to note that likewise strong deviations from present many-body theories were observed in positron annihilation experiments on heavy alkali metals.[9] The breakdown of the above-mentioned theories was also ascribed to strong electron localization.

B. Plasmon half-width

The plasmon half-width at $q = 0$ should be proportional to the square of the V_{110} Fourier coefficient of the pseudopotential,[27] which is the only important one in the alkali metals. This is confirmed by Fig. 9 which was originally proposed by Gibbons and Schnatterly,[50] where the solid circles refer to their measurements and the open circles to ours. We omit error bars for the width since the symbols themselves exceed already the uncertainty of the measurement. At low values of the pseudopotential, our data points level off from the straight line, indicating the influence of others than band-structure effects. Those become more pronounced when the band-structure contribution approaches zero. Probably, the deviations are caused by boundary scattering (the grain size in the Na and K polycrystalline samples was about 200 Å), which gives a lower limit of just the required size for the observed halfwidth.

In Fig. 10 we compare the dispersion of the width calculated in the NFE approximation by Sturm and Oliveira[51] with the measured dispersion. The band-structure contribution decreases with increasing momentum transfer. This results from the fact that the phase space for the plasmon decay into electron-hole excitations decreases quadratically with increasing q. This is indicated by the dashed-dotted line labeled BS in Fig. 10. It is the inclusion of electron-electron scattering which counteracts and which yields in total a net positive in-

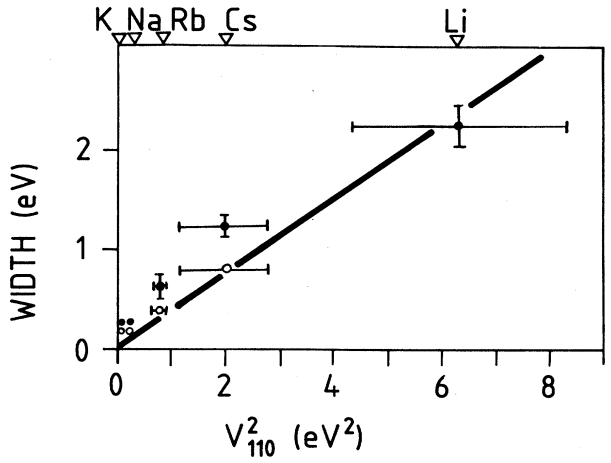

FIG. 9. Measured plasmon linewidth at $q = 0$ of all alkali metals plotted vs the square of the pseudopotential. The points with error bars and the solid line correspond to the measurements and a fit of other authors (Refs. 27, 36, and 37). The open circles represent the results of our measurements.

crease (labeled BS+*CE*). However, the differences between measured and theoretically estimated widths are enormous, in particular for K.

Plasmon half-width in the long-wavelength limit $q=0$ is caused by several mechanisms, like electron scattering with phonons, at grain boundaries or at Bragg planes, which provides the momentum necessary to couple the plasmon to the electron-hole continuum. The latter mechanism is in general the most effective one,[23] and Fig. 9 demonstrates that it also dominates the plasmon half-width of the alkali metals.

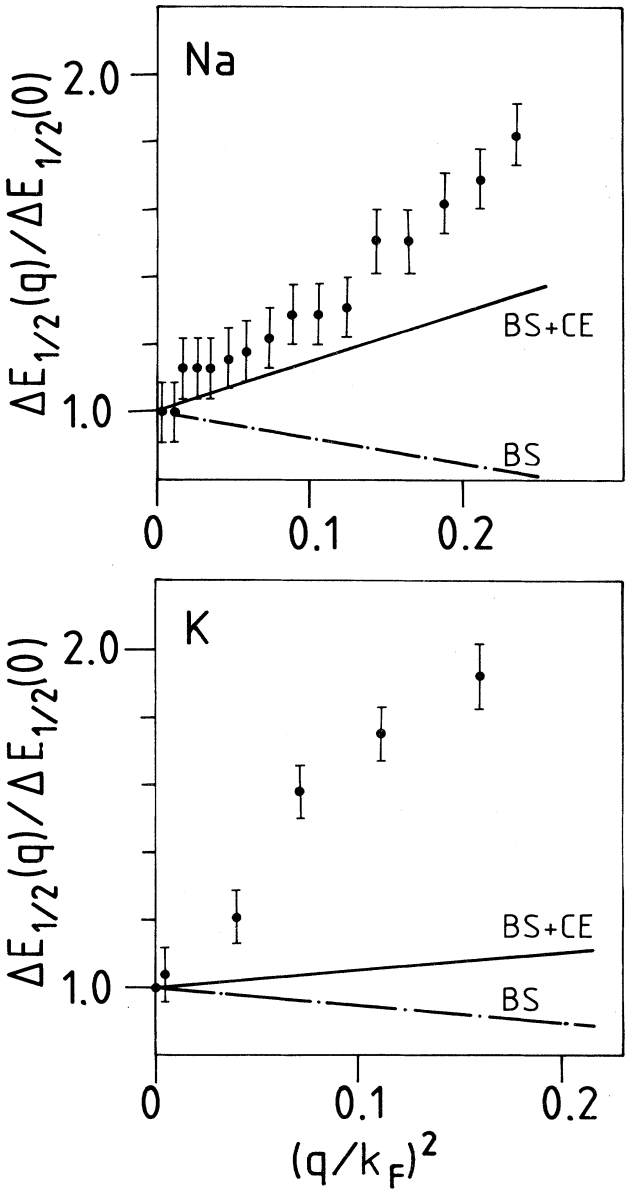

FIG. 10. Comparison of the measured dispersion of Na and K plasmon half-width with theoretical predictions by Sturm and Oliveira (Ref. 51). BS designates the pure band-structure contribution to the plasmon half-width, BS+*CE* represents the total damping when electron-electron scattering is included.

Concerning the plasmon half-width dispersion, all metals investigated so far obeyed a positive, quadratic dispersion for q up to the critical wave vector q_c, beyond which Landau damping sets in and causes a tremendous increase in linewidth. The metal investigated most extensively is Al, where the positive, quadratic dispersion has been successfully explained by the inclusion of band-structure effects.[52] Nevertheless, it is unclear why up to now, in no cubic metal there has been found any anisotropy in plasmon-linewidth dispersion,[23] although it should be expected when band structure controls the dispersion. The situation is even more puzzling in the case of the alkali metals. For Na and K, as shown in Fig. 10, theory predicts too slight a dispersion, for Rb and Cs we estimate that the two contributions, BS and *CE*, nearly cancel. The linear plasmon half-width dispersion of Cs extending beyond q_c is in sharp contrast to the usually encountered quadratic behavior. The $q^{1.5}$ dependence in the case of Rb may be interpreted as a superposition of a linear and a quadratic term. But so far, theory has put forward only one process which provides a linear dependence, i.e., the plasmon decays into another plasmon by means of absorption or emission of a phonon,[53] a process which turns out to be too weak to explain our data. Hence it seems very unlikely that the observed anomalies in the linewidth dispersion can be accounted for by band-structure effects. The influence of low-lying *d* states coming close to the Fermi level in the heavy alkali metals is not clear. Once again we note that we have neither observed any interband transitions into unoccupied *d* states, nor a substantial shift of plasmon energy away from its theoretical value, which would have revealed their relevance.

In K the linewidth increases much faster than in Na. Whereas in the long-wavelength limit the plasmon half-widths are almost identical, at about $q=q_c$, K reaches about twice the Na linewidth. Since both metals have a bcc lattice (we disregard the existence of *d* electrons for the reasons cited above) their band structure is similar on the scale of Fermi momentum (or somewhat less accurately on the scale of critical momentum). This indicates that something beyond band structure comes into play here. Since by going from Na to Cs we strongly enhance the exchange and correlation effects, it does not seem surprising that there is some increasing influence on the plasmon linewidth when turning to the heavier alkali metals. This expected trend is corroborated by the measurements on plasmon dispersion, where we found increasing deviations from RPA with increasing r_s.

The parallelism of the development of plasmon energy of half-width dispersion and in particular the fact that these deviations from RPA are growing when passing from Na to Cs, emphasizes that half-width dispersion, as well, is strongly modified by exchange and correlation. Refined theories for plasmon linewidth dispersion need the inclusion of exchange and correlation. We note that in highly correlated metals the Fermi edge smears out,[47] which makes the electron-hole continuum broaden, so that the critical wave vector is no longer well defined. In principle, this can enhance plasmon decay below q_c, and

also explain the unchanged dispersion of Rb and Cs when passing through q_c.

C. Intraband transitions and zone boundary collective states

In Fig. 5 we have shown experimental spectra of the intraband transitions in Na and Rb, the observation of which is among the first of this kind besides those[29,54] made in Al. The identification of the observed features as intraband transitions is confirmed by the fact that they agree in energy, intensity (relative to the volume plasmon), and in line shape with calculations based on the LM function with the inclusion of LFC by VS.[39] The intraband excitations correspond to single-particle excitations of electrons within the Fermi sphere to unoccupied states outside it. The upper energy cutoff of this feature reflects transitions of electrons at the Fermi surface into unoccupied states with the direction of the measured momentum transfer $\mathbf{q}$ being parallel to the electron's initial momentum $\mathbf{k}_F$. Hence the dispersion of the cutoff energy of the interband transitions directly measures the dispersion of the unoccupied part of the conducting band and is, therefore, related to the effective mass of the electrons in this energy range. The cutoff energies were obtained by a least-squares fit of the data by the function $\mathrm{Im}[-1/\epsilon_{\mathrm{LM\text{-}VS}}(q^*,\omega)]$ yielding the solid lines in Fig. 5. In the case of Na, the only fit parameter was the electron momentum q^*. The damping parameter Γ was estimated from the plasmon linewidth. In the case of Rb, however, it was necessary to optimize besides q^* also the damping parameter Γ. From the difference between q and q^* (measured and fitted momentum transfer) the effective band mass m^* can be derived. The parameters m^* and Γ are listed in Table I.

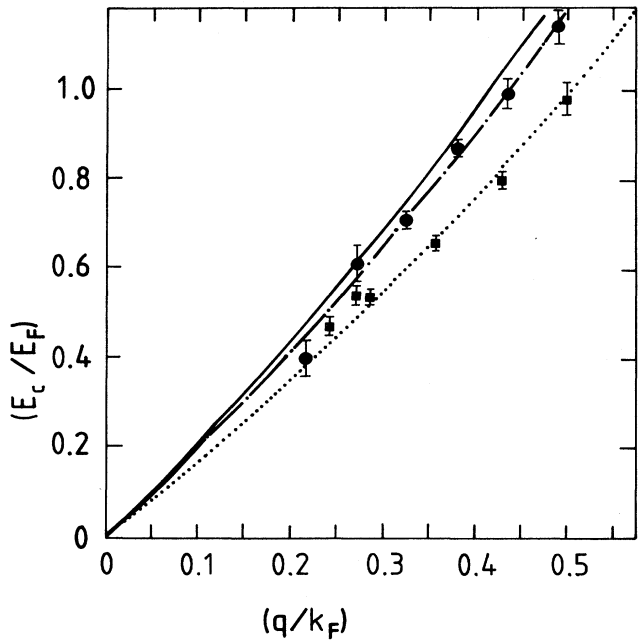

FIG. 11. The dispersion of the upper cutoff energy E_c of intraband transitions (normalized to the free-electron Fermi energy E_F). Symbols with error bars are from fits to the measured spectra, circles are for Na and squares for Rb. Lines are parabolas for free electrons of various band masses, being 1.00 (bold line), 1.05 (dash-dotted line), and 1.25 (dotted line), respectively.

Figure 11 shows a plot of the cutoff energies E_c normalized to the free-electron Fermi energy E_F versus momentum transfer q normalized to k_F derived from the measurements on Na (circles) and Rb (squares). Included are three curves of the form

$$E_c/E_F=(m/m^*)(2q/k_F+q^2/k_F^2)$$

for three different effective masses $m^*/m=1.00$ or 1.05 and 1.25, respectively. The comparison between experimental points and the calculated curves yields for Na an increase of the effective mass of 5% compared to the free-electron band mass.

This result seems to be in conflict with a number of recent publications which indicate a substantial reduction of the Fermi energy corresponding to much higher band masses. Among those are photoemission measurements[11,55] ($m^*/m=1.28-1.18$), x-ray absorption spectroscopy[56] on the K edge of Na ($m^*/m=1.16$), and theoretical calculations including electron self-energy renormalization by Northrup *et al.*[57] ($m^*/m=1.18$) and by Shung *et al.*[58,59] ($m^*/m=1.12$). At first it should be noted that the theoretical calculations have given the band mass of the occupied states, although Northrup *et al.*[57] claim that the band narrowing should persist in the unoccupied states. Also the photoemission yields information on occupied bands while the x-ray absorption results and the present measurements on the energy cutoff of interband transitions yields information on unoccupied states. This is an important point to note since due to the k dependence of the self-energy correction[60] the renormalization of the band mass should be stronger at $k=0$ compared to $k\geq k_F$. A further explanation of the different experimental results of the effective mass may be the different measuring processes. In photoemission, one electron is removed from the conduction band, in x-ray absorption spectroscopy there is the interaction with a localized core hole while in the present intraband transitions the interaction of the excited electron with the hole, i.e., excitonic effects, may be important. At present we have no theoretical explanation why, in the latter measuring process, the effective mass should be close to the free-electron value.

The result of an effective mass close to one is furthermore supported by our measurements of the dispersion of the ZBCS's in Na which were shown in Fig. 6. As pointed out above, they are caused by a combination of intraband and interband transitions into final states near the zone boundary where a gap is opened due to scattering of the electrons by the ion potentials. The loss structure broadens rapidly with increasing momentum transfer q. Theoretically it should retain its sharpness and its intensity should increase with increasing q. That this is not the case is an artifact of our measurements, where we used a single crystal with nonvanishing mosaic spread. Small tilts of the spatial orientation of individual crystallites

correspond to energy shifts of the gap location, which depends on the length of the q-vector projection on the [110] direction. This effect becomes more and more perceptible with increasing q. This is particularly true in the case of Na having a narrow band gap or a weak pseudopotential, respectively. The ZBCS intensity, too, confirms the weakness of the band-structure effects in Na. Nevertheless, the energy of the ZBCS can be determined with good accuracy. The inset in Fig. 6 shows that the measured ZBCS's (dots) are for small q very close to the upper gap edge of the particle-hole continuum (interband transitions) calculated for $m^*/m=1$, and then tend for higher q towards the lower gap edge (intraband transitions) in excellent agreement with predictions by Foo and Hopfield[20] and recent calculations by Sturm and Oliveira.[61] It should be noted here that contrary to the case of the intraband transitions the ZBCS's are a probe of both the unoccupied states (at the zone boundary) and the occupied states. A substantial band narrowing would cause a noticeable shift in the energy and dispersion of ZBCS's. The comparison of the experimental data on ZBCS's with calculations yield an upper limit for the mass enhancement of conduction electrons in Na of 5%. This is in excellent agreement with what we concluded above from the analysis of the intraband transitions. Furthermore, the measurements on the ZBCS's provides evidence that the conduction band is not severely distorted at the Fermi edge as was concluded from the photoemission results. Hence there is also no indication of charge-density waves in Na.

ZBCS's have been previously observed[62,63] in Li and Be using inelastic x-ray scattering. In these metals, ZBCS's are much easier to observe than in Na thanks to the stronger pseudopotential.[64] The fundamental difference between EELS and inelastic x-ray scattering is that the latter is more suitable for the range $q>q_c$, whereas the former is usually a good probe for $q<q_c$, due to the different q dependencies of the cross sections for x rays on one hand and electrons on the other.

The theoretical postulation of the ZBCS and its experimental verification is closely related to the discussion about the influence and the strength of exchange and correlation effects. Depending on the number of nonnegligible pseudopotential coefficients, one might obtain a complete ZBCS band structure,[65] since every pseudopotential coefficient generates a corresponding ZBCS. The smooth electron-hole continuum, as calculated in the RPA, becomes structured. Structures which have been found in the electron-hole continuum and which were interpreted as exchange and correlation effects or even as an indication of an incipient Wigner crystallization[66] are probably caused by band-structure effects.

To close this section we discuss the measurements of the intraband transitions in Rb. An effective mass of $m^*/m=1.25$ has been derived from the comparison of the cutoff energies of the intraband transitions with calculations (see Fig. 11). The 25% increase of the effective mass may be explained by band-structure effects since unoccupied d states come close to the Fermi level in the heavy alkali metals. We cannot exclude exchange and correlation effects from causing the deviation from a free-electron behavior. The fact that the damping constant Γ had to be adjusted separately in the fits, i.e., the damping is different for the plasmon and interband transitions, may support the latter explanation.

VI. CONCLUSIONS

We have provided extensive experimental data on the fundamental excitations of the alkali metals Na to Cs. It turned out that a full understanding of these metals is prevented by unexpectedly strong exchange and correlation effects. The results on the dispersion of plasmon energy and half-width proved to be inconsistent with the predictions of current Fermi-liquid theories. The concept of local field corrections for describing exchange and correlation effects appears to be inadequate for the heavy alkali metals. The strong correlation at low electron densities causes the negative plasmon dispersion in Cs, indicating an incipient instability of its electron fluid. We have also provided data which emphasize that band-structure effects are of minor importance for the alkali metals investigated here and that they are unlikely to account for the observed dispersion anomalies. For the case of Na, we showed that the electron band mass is near unity, as it should be for a NFE metal. In Rb, however, this band mass is enhanced. In Na, the influence of the ion lattice shows up in the existence of the ZBCS, which has a much lower intensity compared to the volume plasmon. Unfortunately, the information that could be obtained for the heavier alkali metals is less reliable. More measurements on single crystals of the heavy alkali metals and the investigation of the Rb and Cs excitation spectra in the momentum range beyond q_c by inelastic x-ray scattering appear to be highly desirable.

ACKNOWLEDGMENTS

We are indebted to H. Rietschel, R. von Baltz, and K. Sturm for continuous interest in this work and to N. Nücker and B. Scheerer for technical support.

*Present address: Bell Telephone Laboratories, Murray Hill, NJ 07974.

[1]M. Springford, I. M. Tempelton, and P. T. Coleridge, J. Low Temp. Phys. **53**, 563 (1983).

[2]S. P. Kowalczyk, L. Ley, F. R. McFeely, R. A. Pollack, and D. A. Shirley, Phys. Rev. B **8**, 3583 (1973); P. Steiner, H. Höchst, and S. Hüfner, in *Photoemission in Solids,* edited by L. Ley and M. Cardona (Springer, Berlin, 1979), pp. 349–362.

[3]L. Oberli, A. A. Manuel, R. Sachot, P. Descouts, and M. Peter, Phys. Rev. B **31**, 6104 (1985).

[4]T. Inagaki, L. C. Emerson, E. T. Arakawa, and M. W. Williams, Phys. Rev. B **13**, 2305 (1976).

[5]R. Garrond and H. Roubaud, Surf. Sci. **146**, 527 (1983).

[6]Å. Fäldt and J. Neve, Solid State Commun. **45**, 399 (1983).

[7]N. V. Smith, Phys. Rev. **183**, 634 (1969).

[8]U. El-Hanany, G. F. Brennert, and W. W. Warren, Jr., Phys.

Rev. Lett. **50**, 540 (1983).
[9]J. Arponen and E. Pajanne, Ann. Phys. (N.Y.) **121**, 343 (1979).
[10]A. W. Overhauser, Adv. Phys. **27**, 343 (1978).
[11]E. Jensen and E. W. Plummer, Phys. Rev. Lett. **55**, 1912 (1985).
[12]A. W. Overhauser, Phys. Rev. Lett. **55**, 1916 (1985).
[13]R. Taylor and A. H. MacDonald, Phys. Rev. Lett. **57**, 1639 (1986).
[14]T. M. Giebultowicz, A. W. Overhauser, and S. A. Werner, Phys. Rev. Lett. **56**, 1485 (1986); **56**, 2228(E) (1986).
[15]L. Pintschovius, O. Blaschko, G. Krexner, M. de Podesta, and R. Currat, Phys. Rev. B **35**, 9330 (1987).
[16]H. You, J. D. Axe, D. Hohlwein, and J. B. Hastings, Phys. Rev. **35**, 9333 (1987).
[17]L. H. Dubois and N. V. Smith, J. Phys. F **17**, L7 (1987).
[18]K. W.-K. Shung and G. D. Mahan, Phys. Rev. Lett. **57**, 1076 (1986).
[19]D. Pines, *Elementary Excitations in Solids* (Benjamin, New York, 1964); for an introduction, see also P. M. Platzman and P. A. Wolff, *Waves and Interactions in Solid State Plasmas* (Academic, New York, 1973).
[20]E.-Ni Foo and J. J. Hopfield, Phys. Rev. **173**, 635 (1968).
[21]A. vom Felde, J. Fink, Th. Bueche, B. Scheerer, and N. Nücker, Europhys. Lett. **4**, 1037 (1987).
[22]J. Fink, Adv. Electron. Electron Phys. **75**, 121 (1989).
[23]H. Raether, in *Excitations of Plasmons and Interband Transitions by Electrons,* Vol. 88 of *Springer Tracts in Modern Physics,* edited by G. Höhler (Springer, New York, 1980).
[24]N. D. Mermin, Phys. Rev. B **1**, 2362 (1970).
[25]For a review of LFC's see, for example, S. Ichimaru, Rev. Mod. Phys. **54**, 1017 (1982).
[26]K. Sturm, Solid State Commun. **48**, 29 (1983).
[27]K. Sturm, Adv. Phys. **31**, 1 (1982).
[28]T. Kloos, Z. Phys. **265**, 225 (1973).
[29]E. Petri and A. Otto, Phys. Rev. Lett. **34**, 1283 (1975).
[30]K. J. Krane, J. Phys. F **8**, 2133 (1978).
[31]H. Moeller and A. Otto, Phys. Rev. Lett. **45**, 2140 (1980); **46**, 789 (1981); **46**, 1707 (1981).
[32]M. S. Haque and K. L. Kliewer, Phys. Rev. Lett. **29**, 1461 (1972); Phys. Rev. B **7**, 2416 (1973).
[33]K. Reichelt, J. Cryst. Growth **19**, 258 (1973).
[34]C. Kunz, Phys. Lett. **15**, 312 (1965).
[35]C. Kunz, Z. Phys. **196**, 311 (1966).
[36]P. C. Gibbons, S. E. Schnatterly, J. J. Ritsko, and J. R. Fields, Phys. Rev. B **13**, 2451 (1976).
[37]S. E. Schnatterly, in *Solid State Physics* edited by H. Ehrenreich, F. Seitz, and D. Turnbull (Academic, New York, 1979), Vol. 34, p. 275.
[38]J. Sprösser-Prou, A. vom Felde, and J. Fink, Phys. Rev. B **40**, 5799 (1989).
[39]P. Vashishta and K. S. Singwi, Phys. Rev. B **6**, 875 (1972).
[40]J. R. Tessmann, A. H. Kahn, and W. Shockley, Phys. Rev. **92**, 890 (1953).
[41]J.-P. Jan, A. H. MacDonald, and H. L. Skriver, Phys. Rev. B **21**, 5584 (1980).
[42]K. Syassen and K. Takamura, in *Solid State Physics under Pressure,* edited by S. Minomura (Terra Scientific, Tokyo, 1985), p. 55.
[43]B. Dabrowski, Phys. Rev. B **34**, 4989 (1986).
[44]K. S. Singwi, M. P. Tosi, R. H. Land, and A. Sjölander, Phys. Rev. **176**, 589 (1968).
[45]M. Taut, Solid State Commun. **56**, 905 (1988).
[46]K. Utsumi and S. Ichimaru, Phys. Rev. A **26**, 603 (1982).
[47]P. Ziesche and G. Lehmann, *Elektronentheorie der Metalle* (Springer, Berlin, 1983).
[48]D. M. Ceperley and B. J. Alder, Phys. Rev. Lett. **45**, 566 (1980).
[49]A. Bagchi, Phys. Rev. **178**, 707 (1969); K. Sturm, Adv. Phys. **31**, 1 (1982).
[50]P. C. Gibbons and S. E. Schnatterly, Phys. Rev. B **15**, 2420 (1977).
[51]K. Sturm and L. E. Oliveira, Phys. Rev. B **24**, 3054 (1981).
[52]K. Sturm, Z. Phys. B **28**, 1 (1977).
[53]M. Hasegawa, J. Phys. Soc. Jpn. **31**, 649 (1971).
[54]M. Urner-Wille, J. Phys. D **10**, 49 (1977).
[55]In-Whan Lyo and E. W. Plummer, Phys. Rev. Lett. **60**, 1558 (1988).
[56]P. H. Citrin, G. K. Wertheim, T. Hashizume, F. Sette, A. A. MacDowell, and F. Comin, Phys. Rev. Lett. **61**, 1021 (1988).
[57]J. E. Northrup, M. S. Hybertsen, and S. G. Louie, Phys. Rev. Lett. **59**, 819 (1987).
[58]K. W.-K. Shung, B. E. Sernelius, and G. D. Mahan, Phys. Rev. B **36**, 4499 (1987).
[59]K. W.-K. Shung and G. D. Mahan, Phys. Rev. B **38**, 3856 (1988).
[60]H. Rietschel and L. J. Sham, Phys. Rev. B **28**, 5100 (1983).
[61]K. Sturm and L. E. Oliveira, Europhys. Lett. **9**, 257 (1989).
[62]W. Schülke, H. Nagasawa, and S. Mourikis, Phys. Rev. Lett. **52**, 2065 (1984); W. Schülke, H. Nagasawa, S. Mourikis, and P. Lanzki, Phys. Rev. B **33**, 6744 (1986).
[63]W. Schülke, U. Bonse, H. Nagasawa, S. Mourikis, and A. Kaprolat, Phys. Rev. Lett. **59**, 1361 (1987).
[64]N. W. Ashcroft, Phys. Lett. **23**, 48 (1966).
[65]K. Sturm and L. E. Oliveira, Phys. Rev. B **30**, 4351 (1984).
[66]P. M. Platzman and P. Eisenberger, Phys. Rev. Lett. **33**, 152 (1974).